Research Paper
Journal of Aerospace System Engineering
Vol.14, No.4, pp.10-17 (2020)
EISSN 2508-7150
http://dx.doi.org/10.20910/JASE.2020.14.4.10

Monte Carlo Simulation of MR Damper Landing Gear Taxiing Mode under Nonstationary Random Excitation

Hyo-Sang Lee[1], Dae-Sung Jang[2] and Jai-Hyuk Hwang[3,†]
[1]Dept. of Aerospace and Mechanical Engineering, Graduate at KAU
[2]Dept of Aerospace and Mechanical Engineering, Korea Aerospace University
[3]Dept of Aerospace and Mechanical Engineering, Korea Aerospace University

Abstract

When an aircraft is taxiing, excitation force is applied according to the shape of the road surface. The sprung mass acceleration caused by the excitation of the road surface negatively affects the feeling of boarding. This paper addresses the verification process of the semi-active control method applied to improve the feeling of boarding. The Magneto−Rheological damper landing gear model is employed alongside the control method. It is a Oleo-Pneumatic damper filled with a fluid having the characteristics of increasing yield stress when subjected to a magnetic field. The control method involves verifying Skyhook Control Type2 developed by Skyhook control. The Sinozuka white noise model that considers runway characteristics was employed for the road surface in the simulation. The runway road surface obtained through this model has stochastic characteristics, so the dynamic characteristics were analyzed by applying Monte-Carlo simulation. A dynamic analysis was conducted by co-simulating the landing gear model made by RecurDyn and the control method designed by Simulink. Simulation results show that the Skyhook Control Type2 method has the best control effect in the low speed range compared to the passive type (without control) and skyhook control.

Key Words: Taxiing Mode, Semi-Active Control, MR Damper, Skyhook Control Type2, White Noise, Monte-Carlo Simulation, Co-Simulation

1. Introduction

Aircraft taxiing on the runway is subjected to irregular excitation depending on the shape of the runway road surface. [1-3]. The acceleration of the upper mass of the aircraft caused by the excitation of the road surface should be improved since it is the main factor that negatively impacts the boarding feeling of passengers and pilots. A previous study reduced the upper mass acceleration by applying the skyhook control method, which is widely used in vehicle suspension systems, to improve the feeling of boarding of aircraft landing gear [4]. However, the control effect is weak when the upper mass velocity is low, which limits the applicability of this method. This is due to the characteristic of skyhook control, which calculates the control by receiving only the upper mass speed. To overcome this limitation, Skyhook Control Type2, which is a control method that additionally feeds back the upper mass acceleration from the existing skyhook control, was devised [5]. To verify the control effect of Skyhook Control Type2, a landing gear model using RecurDyn and a controller designed in Simulink were interlinked and analyzed.

The white noise model proposed by Sinozuka was assumed to describe the characteristics of the runway model [6]. To evaluate the landing process, the run speed was set to decelerate uniformly. The road surface of a runway with constant deceleration can be expressed as a non-stationary random road surface. Because the runway road surface has a stochastic character, uncontrolled and controlled landing gear dynamic characteristics cannot be verified by a definitive analysis method, and Monte-Carlo simulation, a statistical numerical analysis technique, should be used.

To date, several studies on the dynamic characteristics of aircraft landing gear subjected to road excitation have been conducted [7-9]. Although the vibration of the center of gravity of the aircraft and the impact force applied to the landing gear have been reduced by applying proportional–integral–derivative control to active landing gears passing over bumpy roads, their application is limited to bumpy road surfaces [7]. A study analyzing the dynamic characteristics of aircraft landing gear on a non-stationary random road surface with actual runway characteristics was carried out in 1999 [8]. In this study, after modeling the aircraft landing gear as a nonlinear system, the characteristics of the landing gear were statistically identified through Monte-Carlo analysis. However, the landing gear model used in this study was analyzed only under the assumption of non-control as a passive landing gear with a pneumatic-hydraulic structure. A study on vibration control of an active landing gear receiving random excitation has also been conducted [9]. For the study conditions, a statistical analysis was required since a random road surface has a different form for each road surface sample function, but this study did not employ a statistical method. The present study verifies the control characteristics and effects of the

Received: Nov. 07, 2019 Revised: Apr. 02, 2020 Accepted: May 17, 2020
† Corresponding Author
Tel: +82-2-300-0109, E-mail: jhhwang@kau.ac.kr

application of Skyhook Control Type 2 on the semi-active Magneto–Rheological (MR) damper landing gear, in comparison with the passive type (uncontrolled) and the existing Skyhook control gear. To verify the control technique, Monte-Carlo simulation was applied.

The remainder of this paper is structured as follows. In Chapter 2, MR damper landing gear and the model of the runway road surface are described. In Chapter 3, the control logic of Skyhook Control Type 2 is explained. In Chapter 4, by using Monte-Carlo simulation, the control effect of Skyhook Control Type2 is compared with the results of the passive and existing Skyhook technique and the characteristics are verified. Finally, in Chapter 5, summarized results are presented.

2. MR landing gear and runway road surface modeling

2.1 MR damper landing gear modeling

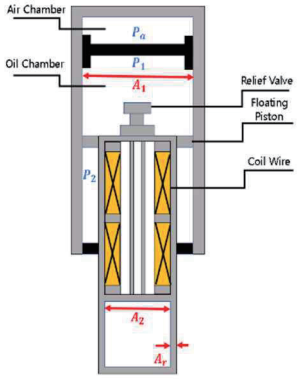

Fig. 1 MR Landing Gear

Table 1 Landing Gear Parameters

Parameter	Symbol	Value	Unit
m_1	**Sprung mass**	680	kg
m_2	**Unsprung mass**	18	kg
A_p	**Piston Area**	0.0013	m^2
P_0	**Initial Pressure**	1.1	$M\,pa$
V_0	**Initial Volume**	3.2×10^{-4}	m^3
n	**Polytropic index**	1.3	
μ_A, μ_B	**Friction Coefficient**	0.1	
D_v	**Offset between Damper & Tire**	0.3	m
D_b	**Offset between Bearing**	0.2	m
T_m	**Tire Stiffness**	412×10^3	N/m
b	**Tire Stiffness index**	1.13	

An Oleo-Pnuematic damper is most frequently used for landing gears and has various structures, but the principle of shock absorption is the same [10-11]. The structure of the landing gear covered in this paper is similar (refer to Fig. 1) to air-hydraulic landing gears. Table 1 illustrates the design parameters of the landing gear [12]. The applied damper is not a general oil damper but an MR damper in which MR fluid is used. When current flows through the coil, a magnetic field is generated, which changes the yield shear stress characteristic of MR fluid; this can absorb shock load more efficiently than passive landing gear. Internal force exerted on the landing gear includes air force F_a, damping force F_h, and friction force F_f. External force includes tire load, F_T. All internal forces applied on a landing gear can be expressed as a function of stroke s. Stroke s is the difference between the upper mass displacement z_1 and the lower mass displacement z_2; stroke can be expressed as Equation (1).

$$s = z_1 - z_2 \tag{1}$$

Prior to expressing the force applied to the landing gear in an equation, the following assumptions are considered: landing gear tires only have elasticity without damping, MR fluid in the damper is an incompressible fluid, and there is no ground friction and rolling friction.

The internal force acting on the MR landing gear F_d can be expressed as follows:

$$F_d = F_a + F_h + F_f \tag{2}$$

A damper contracts when subjected to road surface excitation. At this time, the air in the chamber goes through a polytropic compression process, and air force F_a can be expressed as follows.

$$F_a = A_p[P_0\left(\frac{V_0}{V_0 - A_p s}\right)^n - P_{ATM}] \tag{3}$$

A_p is cross sectional area of piston, P_0 is the initial pressure in the air chamber, V_0 is initial volume of the air chamber, n is polytropic index, and P_{ATM} is atmospheric pressure.

Damping force F_h is divided into damping force due to dynamic pressure drop of MR fluid when no magnetic field is applied when passing through the orifice F_v and additional damping force generated by the formed magnetic field F_{MR}. It can be expressed as Equation (4) [12].

$$F_h = F_v + F_{MR}\,sgn\,(\dot{s}) = C\dot{s} + F_{MR}\,sgn\,(\dot{s}) \tag{4}$$

Here, $sgn\,(\dot{s})$ is a sign function expressed in stroke speed. Regarding the MR damper landing gear covered in this paper, a relief valve structure was adopted. Since opening and closing of the relief valve is determined according to the direction of fluid movement, asymmetry exists in the damping force F_v during tension and compression. The asymmetric damping coefficient C expresses this.

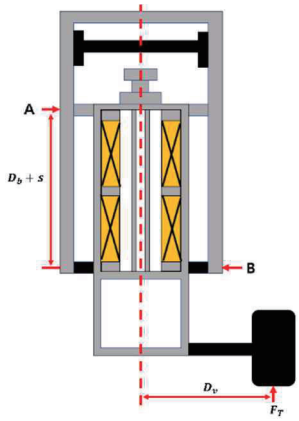

Fig. 2 Friction Force

When a stroke occurs, friction force F_f acts on each bearing due to the offset D_v between the damper's central axis and the tire, as shown in Fig. 2. When moment equilibrium is applied to A and B, which are the areas where frictional force occurs, friction force F_f can be expressed as:

$$F_f = sgn\,(\dot{s})(\mu_A \left|\frac{F_T D_v}{D_b+s}\right| + \mu_B \left|\frac{F_T D_v}{D_b+s}\right|) \quad (5)$$

μ_A and μ_B are the coefficient of friction at A and B, respectively.
Tire load F_T can be expressed in the form of the following exponential function with the assumption that tires only have elasticity without damping [10]:

$$F_T = T_m z_{in}{}^{b} \quad (6)$$

Here, T_m is the coefficient of tire elasticity, z_{in} represents tire deformation, and b is an index of deformation.

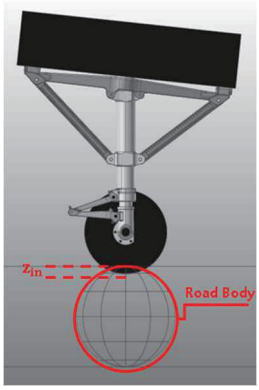

Fig. 3 RecurDyn Model

Fig. 3 shows the landing gear model implemented by RecurDyn. Tire load F_T was simulated with axial force. In this figure, the road body is a dummy body that expresses the shape of the road surface. Tire deformation z_{in} was expressed as an overlap between the road body and the tire on RecurDyn.

2.2 Runway road surface modeling

To analyze the MR damper landing gear taxiing mode through the Monte-Carlo simulation, the runway road surface should be obtained. This can be obtained by selecting a random number that applies the power spectrum density reflecting the runway characteristics. Computer-generated random numbers should have periods, and the number of random numbers used in Monte-Carlo simulation should be less than the period of random number. This guarantees reliable randomness [13].

2.2.1 White noise

The random number applied to Monte-Carlo simulation can be obtained through the white noise model presented by Sinozuka. White noise can be obtained by substituting a random phase angle into the equation presented by Sinozuka. Gaussian random process with zero mean can be expressed as follows [8].

$$w(s) = \sqrt{2}\sum_{k=1}^{N} A_k \cos\,(w_k s - \Phi_k) \quad (7)$$

$$A(k) = [\int_{(k-1)\Delta w}^{k\Delta w} S(w)dw\,]^{\frac{1}{2}} \cong [S(w_k \triangle w)]^{\frac{1}{2}} \quad (8)$$

$$w_k = (k-\frac{1}{2})\Delta w \quad (9)$$

$$\Delta w = \frac{w_u}{N} \quad (10)$$

Here, N is the number of cosine terms, s is a space variable, Φ_k is a random phase angle between $0–2\pi$ with uniform distribution, w_a is cutoff frequency, and $S(w)$ is PSD in which the characteristics of the runway road surface are expressed, as shown in Fig. 4 [14]. By applying the PSD of the runway to the white noise model, a random form of runway road surface can be obtained.

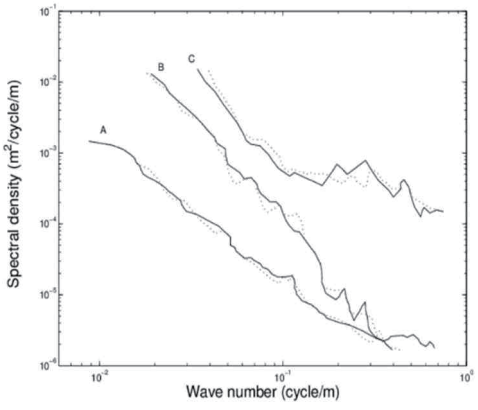

Fig. 4 Spectral densities of roads

2.2.1 Non-stationary runway sample function

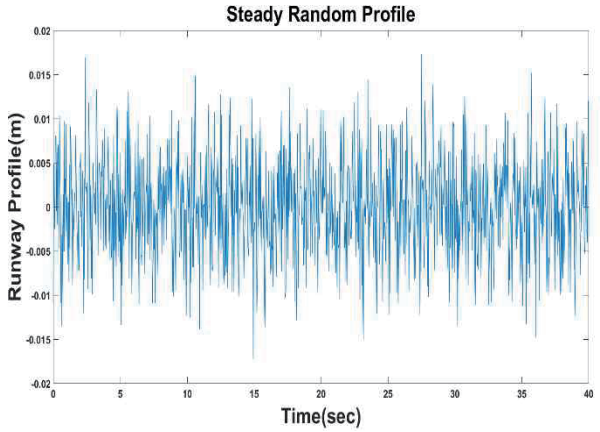

Fig. 5 Steady Random Profile

Fig. 5 is a stationary random road surface function to which the runway characteristic PSD obtained through Equation (7) is applied.

The runway road surface obtained earlier is a stationary random process expressed as a function of runway time. When taxiing at a constant velocity, the stationary random process can be expressed along the time axis, but in this study, it was assumed that an aircraft is grounded on the runway during the landing process. Thus, the situation of taxiing at a constant speed depending on time was applied, which is expressed as a non-stationary random process (i.e., a time-dependent random number).

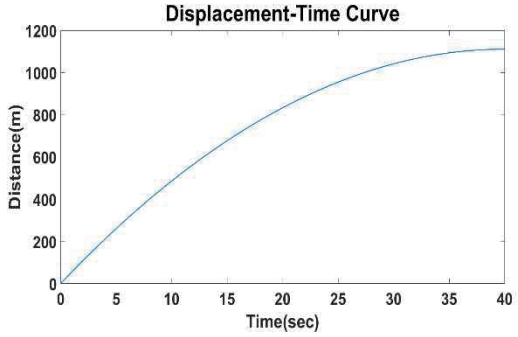

Fig. 6 Displacement-Time Curve

Because the non-stationary random process is a time-dependent function, the stationary random process dependent on distance is expressed as a function dependent on time. Fig. 6 shows the distance over time in the case of constant deceleration from 100 knots (approximately 200 km/h) to a stop over 40 s. If Fig. 6 and Fig. 5, showing a stationary random process, are mapped, a non-stationary random process of the case in which an aircraft taxies at a constant speed can be obtained. The form of the runway with constant deceleration from 100 knots to a stop for 40 s is shown in Fig. 7.

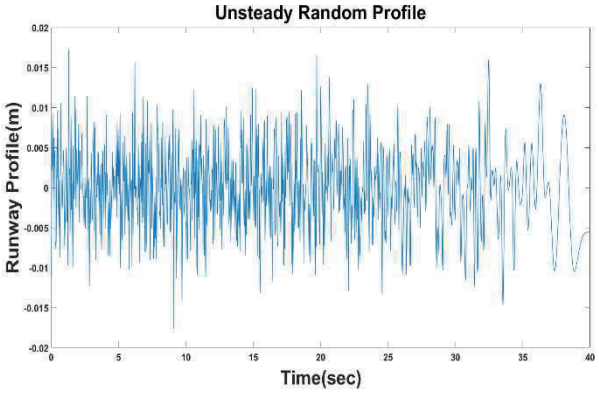

Fig. 7 Unsteady Random Profile

3. Landing gear taxiing mode control method

The degree of boarding feeling can be expressed as the upper mass acceleration. A lower value of upper mass acceleration is associated with improved the feeling of boarding. Skyhook control is a control method that is most commonly applied to improve the feeling of boarding by minimizing the upper mass movement [15]. When skyhook control is applied, upper mass acceleration decreases. However, there is a limitation in that the control effect is poor in sections where the magnitude of the upper mass velocity is small (sections where the sign change of the upper mass velocity occurs) and the magnitude of the upper mass acceleration is large, (sections where the influence of inertia is greater than the motion of the gas). This occurs because the control damping force applied due to the low upper mass velocity also decreases. To overcome the control limitation, Skyhook Control Type2, which additionally feeds back the upper mass acceleration, was devised [5], and the concept map of Skyhook Control Type2 is shown in Fig. 8.

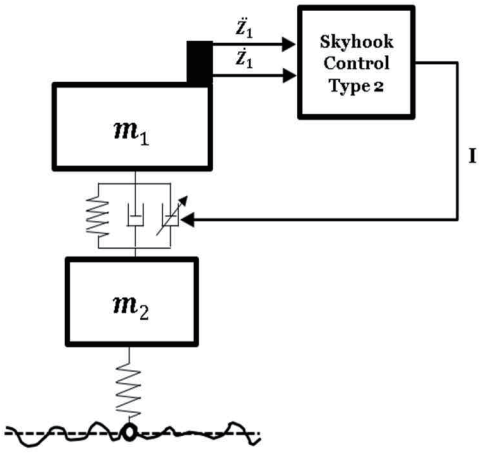

Fig. 8 Skyhook Control Type2

The control damping force can be calculated by receiving the upper mass velocity and acceleration. The MR damper mounted on the landing gear is applied by calculating the

amount of current required to create the control damping force. Skyhook Control Type2's control damping forceF_{Type2} is the sum of the control damping force calculated in the existing Skyhook control method as in Equation (11),$F_{Sky\,hook}$, and control damping force obtained by feedback of upper mass acceleration, F_{acc}.

$$F_{Typ2} = F_{Sky\,hook} + F_{acc} = C_{sky}\,z_1 + C_{acc}\,z_1 \tag{11}$$

There are two control gains, C_{sky}, and C_{acc}, that need to be determined when calculating F_{Type2}. C_{sky} is an optimal control gain determined by the existing Skyhook control method. C_{acc} is the control gain value multiplied by the upper mass acceleration. In the state in which C_{sky} is determined, the control effect is determined as the best case through trial and error.

The MR damper mounted on the landing gear can only absorb vibration energy as a semi-active damper. This means that the control damping force F_{Type2} is valid only in a specific section. The logic for selecting the section in which the control damping force is effective is as follows (refer to Fig. 9).

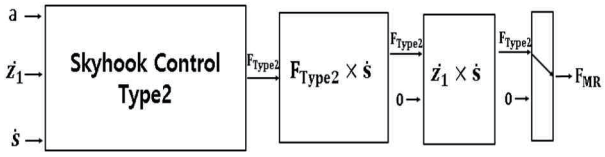

Fig. 9 Controller Flow Chart

F_{Type2}, which was first calculated from Skyhook Control Type2, is applied to the controlled section through two logical terms. The applied logical terms absorb vibrational energy. For first logical term, the MR damping force calculated when the direction of F_{Type2} and $\dot{s}$ coincided, and F_{Type2} is valid. Regarding the second logical term, the MR damping force calculated when the product of $\dot{z}_1$and $\dot{s}$ is positive, and F_{Type2} is valid. Regarding the MR damping force to be applied, F_{MR}, 0 is applied rather than the calculated MR damping force F_{Type2} if either logical term is invalid. In the section where both logical terms are satisfied, the applied MR damping force F_{MR} is determined as F_{Type2}. There is a case in which instantaneous fluctuation in control damping force occurs at a point where the effectiveness changes when taxiing on the random road surface designed. This decreases the control effect by generating chattering in the upper mass acceleration, and accordingly, the control damping force was designed to be smooth by applying the sigmoid function.

4. Monte-Carlo simulation results and discussion

A simulation was performed to evaluate taxiing from 100 knots to a stop over 40 s on non-stationary random road surface modeled in Chapter 2. Whether a control effect is observed depends on how much lower the RMS value of the upper mass acceleration is, compared to the passive type. In order to express the degree to which the RMS value of the upper mass acceleration has decreased compared to the passive type (when not controlled), the performance index J_{RMS} was introduced [16].

$$J_{RMS} = \left[\frac{\sum_{i=1}^{n} \ddot{z}_c(i)^2}{\sum_{i=1}^{n} \ddot{z}_{nc}(i)^2}\right]^{\frac{1}{2}} \times 100(\%) \tag{12}$$

Here, $\ddot{z}_c$ is the upper mass acceleration during control, and $\ddot{z}_{nc}$ represents the upper mass acceleration when uncontrolled. A lower performance index J_{RMS} is associated with a better control effect.

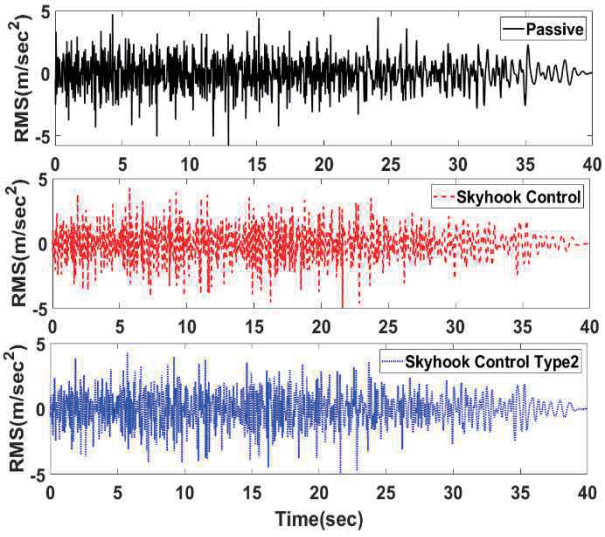

Fig. 10 First Simulation Results

Table 2 Optimum Control Gain Value (50 km/h)

Gain (Type1)	J_{RMS} (%)	Gain (Type2)	J_{RMS} (%)
Passive	100	Type1	99.73
100	99.91	100	99.12
200	99.84	120	98.85
300	99.79	140	98.43
400	99.73	160	98.16
500	Chattering	180	Chattering

Table 3 J_{RMS} of First Simulation

100–0 kn		75–0 kn	
Type	Percent(%)	Type	Percent(%)
Passive	100	Passive	100
Skyhook Control	99.73	Skyhook Control	98.17
Skyhook Control Type2	98.16	Skyhook Control Type2	96.88
50–0 kn		25–0 kn	

Type	Percent(%)	Type	Percent(%)
Passive	100	Passive	100
Skyhook Control	95.91	Skyhook Control	93.48
Skyhook Control Type2	91.16	Skyhook Control Type2	87.20

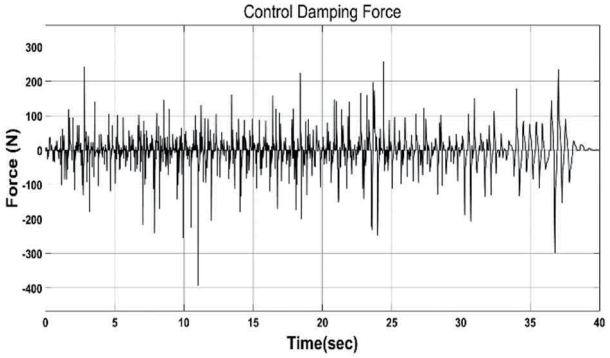

Fig. 11 Control Damping Force

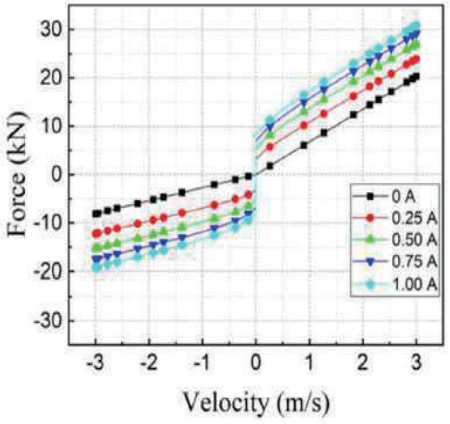

Fig. 12 Force-Velocity of MR Damper

Table 2 presents the simulation results per control gain through the trial and error method of Skyhook Control Type 2. Fig. 10 and Table 3 illustrate the results of the first. They show the results corresponding to passive and each control method in the section ranging from 100, 75, 50, and 25 knots to stop. Skyhook Control Type2 was confirmed to have the best control performance compared to passive and skyhook control in all sections. Fig. 11 is the control damping force when the optimum control gain value is applied. This is a value included in the available range of the control damping force of the MR damper (refer to Fig. 12) [17].

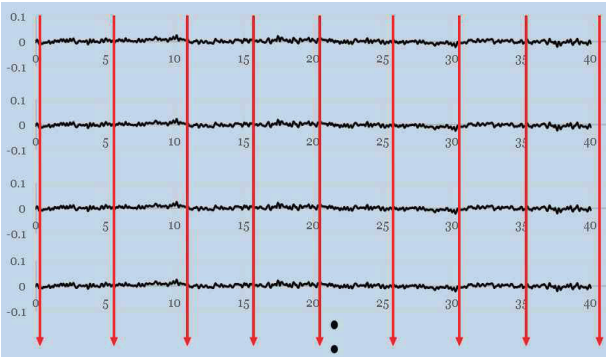

Fig. 13 Matrix of the Monte-Carlo Simulation

Because the runway road surface is a non-stationary random process, the shape of the road surface continuously changes every time a sample function is extracted. Therefore, because it cannot be interpreted in a definitive way, Monte-Carlo simulation is the most suitable analytic method. As shown in Fig. 13, a Monte-Carlo simulation was conducted by statistically processing 1000 non-stationary random process samples in ensemble dimension (by time step).

The number of Monte-Carlo simulations proceeded to the number of times at which the statistical convergence of the simulation is guaranteed. For statistical convergence, a method that verifies the convergence by deriving the variance value of the upper mass acceleration $\mathrm{VAR} = \mathrm{E}[|\ddot{z}_1| - \mathrm{E}(|\ddot{z}_1|)^2]$ for each time step was employed. When the variance value for each time step converged at a certain number of simulations, the statistical characteristics do not change even if additional simulations are performed afterwards; accordingly, the reliability of the results can be determined. Because there is a possibility that the results of each sample function may cancel each other, statistical processing was performed using the absolute value of the upper mass acceleration. When the simulation was run with 1000 sample functions, variance values converged as shown in Fig. 13. Simulation results are shown in Fig. 15–16, and Table 3.

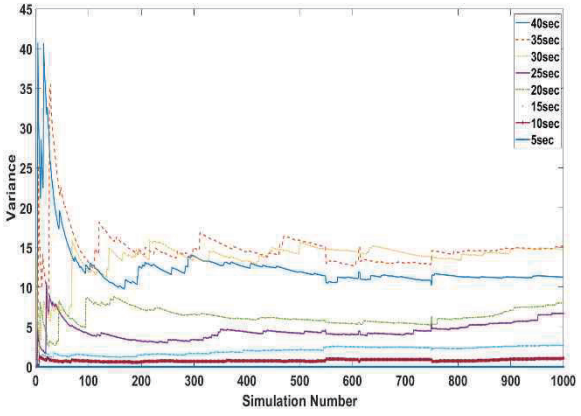

Fig. 14 Variance at 5 s intervals

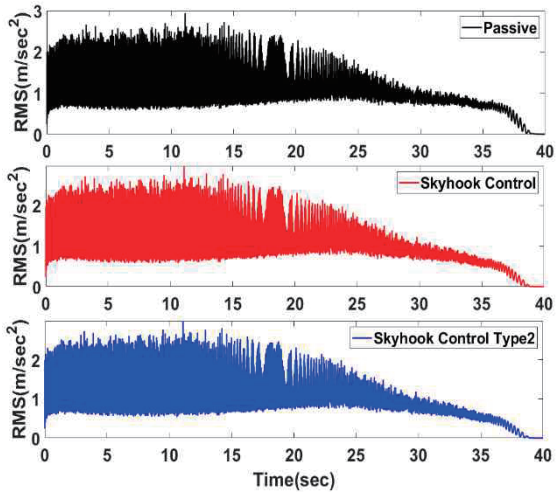

Fig. 15 Result of 1000 Simulations

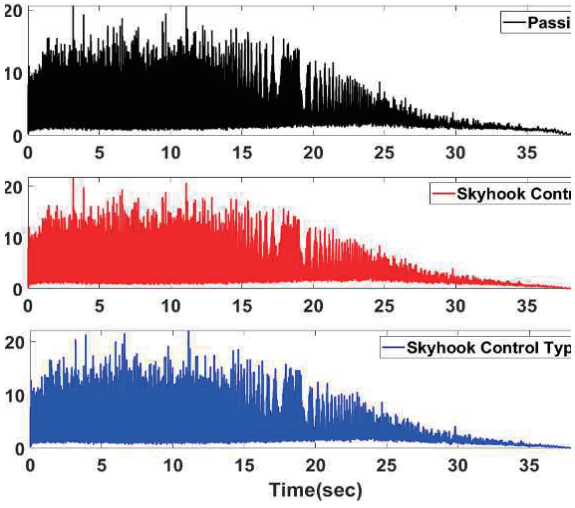

Fig. 16 Variance of 1000 Simulations

Table 4 J_{RMS} of Monte-Carlo Simulations

100–0 kn		75–0 kn	
Type	**Percent (%)**	**Type**	**Percent (%)**
Passive	**100**	**Passive**	**100**
Skyhook Control	**98.78**	**Skyhook Control**	**97.78**
Skyhook Control Type2	**97.27**	**Skyhook Control Type2**	**96.28**
50–0 kn		**25–0 kn**	
Type	**Percent (%)**	**Type**	**Percent (%)**
Passive	**100**	**Passive**	**100**
Skyhook Control	**95.77**	**Skyhook Control**	**93.43**
Skyhook Control Type2	**92.18**	**Skyhook Control Type2**	**87.03**

The Monte-Carlo simulation of MR damper aircraft landing gear taxiing on a non-stationary random road surface yielded similar results to that of the first simulation; Skyhook Control Type2 was found to have the best control effect compared to passive and skyhook control. This is because the control damping force obtained by additionally receiving the upper mass acceleration from Skyhook Control Type 2 compensates for the section where the control effect is poor due to low upper mass velocity. As shown in Fig. 15–16 and Table 4, the control effect that was weak in the high-speed range increased as it transitioned to the low-speed range, and the variance value decreased. This occurred because the frequency of excitation transmitted from the road surface is determined by the aircraft's run speed. Because the excitation of the road surface has a high frequency in the high-speed taxiing area, the external force applied to the landing gear is also a high-frequency input. Since landing gear acts like a low-pass filter, upper mass displacement is characterized by the removal of high-frequency components, while lower mass displacement can hardly filter the excitation force on the road surface [4]. This difference in dynamic characteristics between the upper and lower mass displacement leads to frequent sign changes of the stroke, which causes the control effectiveness to vary, and this limits the area where the control is in effect. The small section where the control is in effect is transferred to the uncontrollable area before sufficient damping force is applied. Thus, it is impossible to apply sufficient control damping force, which decreases the control effect.

5. Conclusion

Aircraft taxiing on the runway is subjected to excitation from the road surface. The acceleration of the upper mass caused by the excitation hinders the feeling of boarding. When skyhook control, which is widely used in automobile suspension, was applied to improve the feeling of boarding, The boarding feeling was improved. However, the control effect is weak because sufficient control damping force cannot be applied in the section with low upper mass velocity. To solve this, Skyhook Control Type 2, which feeds back the upper mass acceleration, was applied.

The white noise model suggested by Sinozuka was used to design the runway road surface, and the characteristics of the runway were taken into account. The sample runway surface obtained through this has a probabilistic property, and accordingly, Monte-Carlo simulation, which is a statistical analysis method, should be applied. The number of simulations and the number of sample functions were set to

1000, and this was determined by checking the statistical convergence of the simulation.

As a result of the simulation, Skyhook Control Type2 was confirmed to have the lowest performance index than the passive type (when not controlled) and Skyhook control; this indicates that the control effect is excellent. Fig. 15–16 and Table 4 show that there is no significant difference compared to the passive type in the high speed range. The control effect in the high-speed range does not differ significantly from the passive type because the excitation force transmitted from the road surface is high frequency input when an aircraft is taxiing at a high speed; accordingly, the controlled section is limited due to frequent fluctuation in control effectiveness. Thus, even before the control damping force is sufficiently applied, it becomes uncontrolled, weakening the control effect. However, the control effect of Skyhook Control Type2 was confirmed to be remarkable in the low-speed range. Particularly, in the case of skyhook control compared to the passive type at 25–0 knots, the J_{RMS} was 93.43%, indicating an improvement of approximately 6%. In the case of Skyhook Control Type2, J_{RMS}= 87.03%, which is an improvement of 13%. The results of the Monte-Carlo simulation on the feeling of boarding improvement with landing gear taxiing on a non-stationary random road surface confirm that Skyhook Control Type2 exhibits the best control effect compared to passive and skyhook control.

Epilogue

This study was carried out with the support of the Korea Evaluation Institute of Industrial Technology as part of the “Aerospace part technology development project (10073291)” of the Ministry of Trade, Industry and Energy. Thank you for the support.

References

[1] D. Yadav and M. C. Nigam, "Ground Induced Non-stationary Response of Vehicles," *Journal of Sound and Vibration*, vol. 61, no. 1, pp. 117-126, 1978.

[2] T. T. Soong and M. Grigoriu, Random Vibration of Mechanical and Structural Systems, Prentice-Hall, 1993.

[3] K. Sobczyk, D. B. Macvean, and J. D. Robson, "Response to Profile Imposed Excitation with Randomly Varying Traversal Velocity,” *Journal of Sound and Vibration*, vol. 52, no. 1, pp. 37-49, 1977.

[4] H. S. Lee and J. H. Hwang, "A study on the taxing mode control technique of MR damper landing gear,” *The Society for Aerospace System Engineering 2018 Spring Conference*, pp. 232-234, April 2018.

[5] H. S. Lee and J. H. Hwang, "A Study on the Taxing Mode Control Technique of Landing System with MR Damper,” *The Society for Aerospace System Engineering 2019 Spring Conference*, April 2019.

[6] M. Sinozuka, "Monte Carlo solution of Structural Dynamics," *Computers & Structures*, vol. 2, pp. 855-874, 1972.

[7] H. Wang, J.T. Xing, W.G. Price, and W. Li, "An investigation of an active landing gear system to reduce aircraft vibrations caused by landing impacts and runway excitations," *Journal of Sound and Vibration*, vol. 317, pp. 50-66, 2008.

[8] J. S. Park, “Dynamic Analysis of Aircraft Landing Gear under Nonstationary Random Excitation Using Nonlinear Model,” MS Thesis, Korea Aerospace University, Gyeong-gi, Republic of Korea, 1999

[9] S. Sivakumar and A. P. Haran, "Mathematical model and vibration analysis of aircraft with active landing gears," *Journal of Vibration and Control*, vol. 21, pp. 229-245, 2015.

[10] B. Milwitzky and F. Cook, "Analysis of Landing Gear Behavior," NACA TN 2755, 1952

[11] N. Currey, "Aircraft Landing Gear Design Principles and Practices," AIAA Education Series, 1988

[12] J. M. Tak, L. Q. Viet, and J. H. Hwang, “Hybrid Control of Aircraft Landing Gear using Magnetorheological Damper” *Journal of Aerospace System Engineering*, vol. 12, no. 1, pp. 1-9, February 2018.

[13] N. C. Nigam and S. Narayanan, Application of Random Vibrations, Addison-Wesley, 1994.

[14] H. Akcay, S. Turkay, A. Mugan, Aand . Kanbolat, "Stochastic Road and Track Modeling," *14th IFAC Symposium on System Identification*, Bewcastle, Australia, vol. 39, pp. 1370-1375, 2006.

[15] D. Karnopp, M. J. Crosby, and R. A. Harwood, "Vibration Control Using Semi-Active Force Generators," *Journal of Engineering for Industry*, vol. 96, no. 2, pp. 619-626, 1974.

[16] K. G. Sung and S. B. Choi, "Ride Comfort Evaluation of Electronic Control Suspension Using a Magneto-rheological Damper,” *The Korean Society for Noise and Vibration Engineering*, vol. 23 no. 5, pp. 463-471, 2013.

[17] C. Han, B. G. Kim, B. H. Kang, and S. B. Choi, "Effects of magnetic core parameters on landing stability and efficiency of magnetorheological damper-based landing gear system,” *Journal of Intelligent Material Systems and Structures*, vol. 31, pp. 198-208, January 2020.